Investigation of Effect of Various Hot Gas Atomisation and Melting Pot Temperatures on Tin Alloy Powder Product

(Kajian Kesan Pelbagai Pengatoman Gas Panas dan Suhu Periuk Lebur pada Produk Serbuk Aloi Timah)

Abdul Basyir[1,*], Robby Kurnia[1], Cherly Firdharini[1,2], Didik Aryanto[1], Wahyu Bambang Widayatno[1,3] &
Agus Sukarto Wismogroho[1,3]

[1]Research Center for Physics, National Research and Innovation Agency, Indonesia
[2]Chemistry Department, Indonesia University, Indonesia
[3]Pusat Kolaborasi Riset Logam Timah, Indonesia

ABSTRACT

This research investigates the effect of different types of hot gas atomisation (argon, nitrogen and oxygen) and melting pot temperatures on the particle size distribution, microstructure, density and phase of tin alloy (Sn-Cu-Ni-Ge) powder products. The tin alloy powder produced by hot argon gas atomisation had the greatest density (7.84 g/cm³) and the most spherical shape. While the tin alloy powder generated by hot oxygen gas atomisation had the lowest density (6.83 g/cm³), the highest endothermic area (60.41695 area unit) and the most elongated, irregular shape. Hot argon and nitrogen gas atomisation at a melting pot temperature of 800 °C produced a higher yield of 0-25 µm powder than at 700 °C. By contrast, hot oxygen atomisation produced the opposite result. However, all the powder products prepared at 800 °C had a higher spherical shape ratio in the range of 0-25 µm. Tin alloy powder produced by hot oxygen gas atomisation comprised only the elements of Sn and Cu, while the powder generated by hot argon and nitrogen gas atomisation consisted of elements such as the ingot of this powder.

Keywords: Density; hot gas atomization; microstructure; particle size; tin alloy powder

ABSTRAK

Penyelidikan ini mengkaji kesan pelbagai jenis pengatoman gas panas (argon, nitrogen dan oksigen) dan suhu periuk lebur pada taburan saiz zarah, struktur mikro, ketumpatan dan fasa produk serbuk aloi timah (Sn-Cu-Ni-Ge). Serbuk aloi timah yang dihasilkan oleh pengabusan gas argon panas mempunyai ketumpatan terbesar (7.84 g/cm³) dan bentuk paling sfera. Manakala serbuk aloi timah yang dijana melalui pengabusan gas oksigen panas mempunyai ketumpatan terendah (6.83 g/cm³), kawasan endoterma tertinggi (60.41695 unit kawasan) dan bentuk paling memanjang dan tidak sekata. Pengatoman argon panas dan gas nitrogen pada suhu periuk lebur 800 °C menghasilkan hasil serbuk 0-25 µm yang lebih tinggi daripada pada 700 °C. Sebaliknya, pengatoman oksigen panas menghasilkan keputusan yang bertentangan. Walau bagaimanapun, semua produk serbuk yang disediakan pada 800 °C mempunyai nisbah bentuk sfera yang lebih tinggi dalam julat 0-25 µm. Serbuk aloi timah yang dihasilkan melalui pengatoman gas oksigen panas hanya terdiri daripada unsur Sn dan Cu, manakala serbuk yang dihasilkan oleh pengatoman argon panas dan gas nitrogen terdiri daripada unsur seperti jongkong serbuk ini.

Kata kunci: Keamatan; mikrostruktur; pengatoman gas panas; serbuk timah paduan; ukuran zarah

INTRODUCTION

The powder metallurgy method is used widely nowadays and has increased over time. Powder metallurgy was chosen over the conventional method because of its ability to produce complex metal with a high-quality product. It is capable of producing a desired shape and quality of metal due to its use of a metal powder that can be processed by various techniques such as injection moulding, forging, hot isostatic pressing, and additive manufacturing. Each technique requires metal powder with different minimum qualities and parameters.

Metal powder production is generally influenced by two aspects: cost and quality requirement. Thus, in satisfying both aspects, many producers have developed products that are cost-effective and possess the physical and chemical characteristics for various applications. Four different methods can be used to produce metal powder, namely atomisation, chemical decomposition, ball milling, and electrolysis (Neikov et al. 2009). Powders are often produced using the atomisation process. Here, based on the spraying principle, gas, water, plasma or a combination is sprayed, sometimes using centrifugal force, onto flowing molten metal in either a vertical or horizontal direction to break it up into fine droplets (Akkas & Boz 2019). Water or gas atomisation is generally preferred for producing powder at high capacity and low cost (Anderson & Terpstra 2002). However, the water atomisation process is less effective at producing powders with good purity (Zhang et al. 2015). Gas atomisation, in contrast, generates smooth, spherically shaped powder, encourages rapid solidification of small-diameter powders, enables serial production and does not alter the chemical composition of the molten metal (Kaysser et al. 2000). Additionally, while the combined atomisation method produces a small particle size, it also requires relatively more equipment, resulting in higher costs. Similarly, plasma atomisation can produce spherical powders but is also characterised by its lower productivity and higher costs compared to the other methods, while the centrifugal atomisation method requires a high rotational speed to produce good powders (Plookphol et al. 2011). As such, gas atomisation is the more effective and efficient method in terms of the cost and production of fine powder.

Tin powder is widely used in the production of self-lubricating bronze bearings and is an element in soldering and brazing paste. As a metal, tin has a low melting point (232 °C) but a high vapour point (2.602 °C); this makes the manufacture of tin powder possible as one alternative to producing smaller and spherical shapes using the principle of melting (liquid). Hence, hot gas atomisation technology was chosen in this experiment.

Previous experiments on tin and tin alloy employing various methods and parameters have been conducted, along with an exhaustive investigation of the characteristics of powder products. Generally, four atomisation types have been used to investigate the morphology, phase transformation and particle size distribution of tin or tin alloy powder: centrifugal atomisation (Xie et al. 2004; Zhang & Zhao 2017), ultrasonic atomisation (Wisutmethangoon et al. 2011), hybrid atomisation that combines gas atomisation and centrifugal atomisation

(Minagawa et al. 2005), and gas atomisation. For gas atomisation, in particular, the parameters of altering the type of gas have been commonly analysed. The various types of gas atomisation that have been applied include pure nitrogen gas for tin (Metz et al. 2008; Özbilen et al. 1996), copper, zinc, magnesium, iron, aluminium alloy (Özbilen et al. 1996; Urionabarrenetxea et al. 2021), tin alloy (Al-Sn-Cu) (Kong et al. 2007) and austenitic steel (Gao et al. 2021; Urionabarrenetxea et al. 2021); pure argon or inert gas for austenitic steel (Gao et al. 2021), tin alloy (Sn-Cu) (Pan et al. 2019; Urionabarrenetxea et al. 2021) and tin alloy (Al-Sn-Cu) (Zhao et al. 2008); pure helium gas for pure metal (Cu, Sn and Fe), tin alloy (Cu-Sn) and stainless steel 316L (Urionabarrenetxea et al. 2021); and a combination of oxygen and nitrogen gas for aluminium (Özbilen et al. 1989).

Based on this literature review, it is evident that the comparison characteristics of tin alloy (Sn-Cu-Ni-Ge) powder produced by three different hot gas atomisers – namely nitrogen, oxygen and argon – have not been analysed, notably atomisation using oxygen as the gas atomiser. The present research therefore aims to investigate the powderisation of tin alloy using a hot gas atomisation system with different gas atomisation types (nitrogen, oxygen and argon) and diverse melting pot temperatures, while keeping the pressure and temperature of the gas constant. Specifically, solid tin alloy is used as the input material for this atomisation experiment. This alloy is one of the primary compositions used for solder paste in the electronics area. The effect of gas atomisation type on powder size distribution (particularly for the size of 0-25 µm), powder shape, density, thermal behaviour and the phase of powder product are clarified and discussed.

MATERIALS AND METHODS

This research used an experimental method, namely the hot gas atomisation experiment; Figure 1 shows the design of the atomisation system. The hot gas atomisation system comprises several main components: (1) the temperature control machine, (2) melting pot, (3) gas source system, (4) gas heating chamber, (5) main atomisation chamber, (6) powder collection chamber and (7) air suction machine. Furthermore, this research applied different melting pot temperatures and types of gas atomisation. The pressure and temperature parameters of the atomisation gas were kept constant.

This research began by preparing all of the equipment and material as shown in Figure 1. The temperature controller was used to set the temperature of the melting pot and atomisation gas chamber. The

melting pot was adjusted to three temperatures, 700, 750 and 800 °C, while the atomisation gas chamber was set at a temperature of 200 °C. Next, 50 grams of tin alloy (tin (99.3 wt.%) – copper (0.7 wt.%) – nickel (0.05 wt.%) – germanium (0.0007 wt.%)) was added to the melting pot. This input material was then melted and the hot gas began to flow through the atomisation chamber. The gate between the melting pot and atomisation chamber was opened, and the hot gas atomisation pulverised the melted tin alloy. Finally, the tin alloy powder was collected in the powder collection chamber. Nitrogen, oxygen and argon were also used alternately in the hot gas atomisation in this research.

The tin alloy powder produced from this system was sieved into four categories, 0-25, 25-40, 40-150 and > 150 µm. When the powder had been sieved, the effects of the various melting pot temperatures and gas atomisation types on the size distribution and particle size of the powder product were analysed and plotted. Furthermore, measurement of the density, endothermic area and phase of the power product was performed for the tin alloy powder with a size of 0-25 µm that resulted from a melting pot temperature of 800 °C.

Scanning Electron Microscope – Energy Dispersive X-Ray Spectroscopy (SEM-EDS) (Hitachi SU-3500 type)

was used to observe the morphology, particle shape and semi-quantitative element of the powder product. Meanwhile, to observe the phase, X-Ray Diffraction (XRD) Rigaku Smartlab with an A-26 CuKα X-ray tube was used. The XRD measurement was set with a step width of 0.01 degrees, a scan speed of 5.0985 degrees per min, a range of 0 – 110 degrees, a voltage of 40 kV and a current of 30 mA. In addition, the density of the powder was measured using the IWAKI PICNO-5M Pycnometer, while the enthalpy process and endothermic area of the powder product were performed by the P2F type of Differential Thermal Analysis (DTA). The DTA test was run in a heating room comprising air gas, with a temperature of 30 to 800 °C, a heating rate of 2.5 °C/min and alumina material as the reference tube.

Image-J software was used to calculate the number of spherical shapes in each powder. Various prior studies have also used this software to count the number of particles in powders (Vandel et al. 2020; Vippola et al. 2016), and the result is reliable. The number of tin particles of 40-150 µm size was used as the reference for the total number of particles calculated. Therefore, the total number of particles size that was measured for sizes of 0-25 µm and 25-40 µm is the same as the total number of particles in 40-150 µm size.
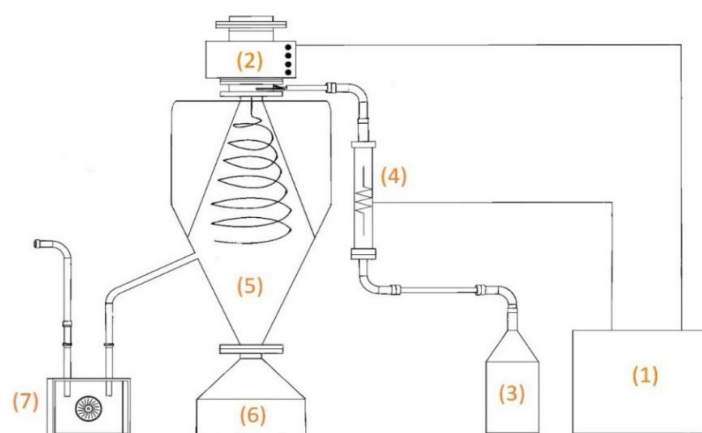

FIGURE 1. Design of gas atomisation system in this experiment

RESULTS AND DISCUSSION

EFFECT OF MELTING POT TEMPERATURE VARIATION ON POWDER SIZE DISTRIBUTION

Figure 2(a) shows the correlation between powder size and various melting pot temperatures with the same hot gas atomisation. Hot nitrogen gas atomisation at a melting pot temperature of 800 °C generated the largest quantity in the 0-25 and 25-40 µm sizes, while the temperature of 700 °C yielded the greatest quantity in the ≥ 40 µm size. A similar phenomenon was identified for tin powder that was generated using hot argon gas atomisation; here,

however, while the greatest quantity was found for the ≥ 40 µm size, this was at a melting pot temperature of 750 °C. Furthermore, a larger quantity of tin powder in the 0-25 µm size was produced from hot argon compared to hot nitrogen gas atomisation.

The opposite result was produced when using hot oxygen gas atomisation, where the largest quantity, namely particles of 0-25 µm in size, resulted from a melting pot temperature of 700 °C, while the largest yield produced at 800 °C was in the ≥ 40 µm size. This reverse phenomenon relating to the size of the tin powder yielded by hot oxygen gas atomisation has been shown to promote the potential enhancement of oxygen existence in the droplet, increasing the viscosity of the molten tin alloy and powder size (Gao et al. 2019). The emergence of tin oxide as an oxidation product may increase at the temperature of 800 °C.

A special case was identified linked to the melting pot temperature of 800 °C, whereby a greater quantity of powder in the 0-25 µm size was produced using hot nitrogen and argon gas atomisation compared to hot oxygen gas. The powder size that resulted from the gas atomisation process was strongly affected by the surface tension and kinematic viscosity at the melting temperature of the metal. The increase in the melting pot temperature thus led to a decrease in the viscosity of the molten metal (Chhabra & Sheth 1990; Feng et al. 2021). Furthermore, an increase in melting pot temperature led to a reduction in cohesion, which then reduced the viscosity and surface tension of the molten metal (Tanaka & Hara 1997). The relationship between the surface tension (σ_m) and the temperature of the molten metal can be expressed by equation (1) (Gao et al. 2019).

$$\sigma_m \left(\frac{M}{\rho_m} \right)^{-\frac{2}{3}} = K \left(T_c - T \right) \qquad (1)$$

where M is the molar mass of the molten metal; T_c is the critical temperature; ρ_m is the melted density; and K is the experimental constant. It can be seen that the surface tension of the molten metal decreases as the temperature increases. The melt kinematic viscosities (η_m) can be defined as

$$\eta = \frac{h}{v_m} \exp \left(\frac{\varepsilon}{kT} \right) \qquad (2)$$

where η is viscosity; h is Planck's constant; v_m is flow unit volume; ε is the activation energy to move the flow unit in the melt; k is the Boltzmann constant; and T is the absolute temperature (Nishimura et al. 2002). Therefore, viscosity and surface tension are strongly

influenced by the melting pot temperature. Reduced viscosity in the molten tin alloy decreases the friction between the alloy and the melting pot wall when the molten alloy flows to the main atomisation chamber. This causes the droplets from the melt to break up more easily into smaller powders.

EFFECT OF GAS ATOMISATION TYPES ON POWDER SIZE DISTRIBUTION

Figure 2(b) shows the relation between the distribution of powder sizes and various hot gas atomisation with the same melting pot temperature. It can clearly be seen that at a melting pot temperature of 700 °C, hot oxygen gas atomisation produced the largest quantity of tin alloy powder with a size of 0-25 µm, while the largest amounts of powder in the 25-40 µm and ≥ 40 µm sizes were generated by hot argon and nitrogen gas atomization, respectively. A similar result was found for the melting pot temperature of 750 °C, where hot oxygen and nitrogen gas atomisation produced the largest quantities of tin powder for the sizes of ≤ 40 and ≥ 40 µm, respectively. While for the melting pot temperature of 800 °C, hot argon gas atomisation produced the most powder with a size smaller than 40 µm, and hot oxygen gas atomisation yielded the largest quantity in the ≥ 40 µm size.

Generally, hot nitrogen gas atomisation produced the lowest quantity of tin alloy powder with a size of 0-25 µm at all melting pot temperatures. By contrast, it produced the greatest amount of tin alloy powder with a size of more than 40 µm at the melting pot temperatures of 700 and 750 °C. Moreover, hot oxygen gas atomisation yielded the greatest quantity of the same powder in the 0-25 µm size at melting pot temperatures of 700 and 750 °C, while hot argon gas atomisation generated the largest quantity at 800 °C. Furthermore, the greatest yields of tin alloy powder in the 25-40 µm size were produced using different melting pot temperatures and gas atomisation types. Thus, at a melting pot temperature of 700 °C, hot argon gas atomisation produced the highest quantity, while hot oxygen and nitrogen gas atomisation generated the maximum quantities of this size at melting pot temperatures of 750 and 800 °C, respectively.

The kinetic energy of the gas (i.e., argon, oxygen and nitrogen) and the viscosity level of melting tin were found to have the greatest effect on powder size distribution. The density of the gas affects the kinetic energy produced by the gas atomisation when impacting the liquid tin alloy. The greater the density, the greater the kinetic energy generated. This increases the probability of obtaining a greater quantity of powder with a small

size. Another parameter, namely velocity, also affects the kinetic energy result. The thermal velocity of hot gas atomisation in this research is calculated using equation (3).

$$v_{th} = \sqrt{\frac{3k_B T}{m}}$$ (3)

where k_B is the Boltzmann constant (1.380649×10^{-23} J/K); T is the temperature (Kelvin); and m is the mass of a particle, in which the mass of argon, oxygen and nitrogen gas is 6.63×10^{-26}, 5.31×10^{-26} and 4.65×10^{-26} kg, respectively. The calculation results of thermal velocity at a temperature of 200 °C (hot gas temperature) are 543.451, 607.202 and 649.126 m/s for argon, oxygen and nitrogen gas, respectively.

In addition, the gas density was calculated using an exponential equation based on experimental data from Younglove and Olien (1985), where the densities of

argon, oxygen and nitrogen gas at 200 °C were 12.207, 9.779, and 8.329 kg/m³, respectively. The results showed that oxygen has the greatest kinetic energy. This is supported by the results in this study, in which more powder under 25 mm in size was produced through the gas atomisation process with hot oxygen gas at a melting pot temperature of 700 °C. It is also supported by the fact that oxygen has a higher entropy value than argon (Drellishak et al. 1964). So, the molten tin alloy will be more exothermic if atomised by hot oxygen gas than by hot argon gas. However, this effect can be minimised by reducing the viscosity of the melting tin. Besides that, the presence of oxygen can increase the viscosity of the molten metal (Gao et al. 2019); thus, at the melting pot temperature of 750 °C, the gap of the powder in this size decreases, and the amount of powder (0-25 μm) produced from hot argon gas atomisation can exceed that produced from hot oxygen gas atomisation at the melting pot temperature of 800 °C.

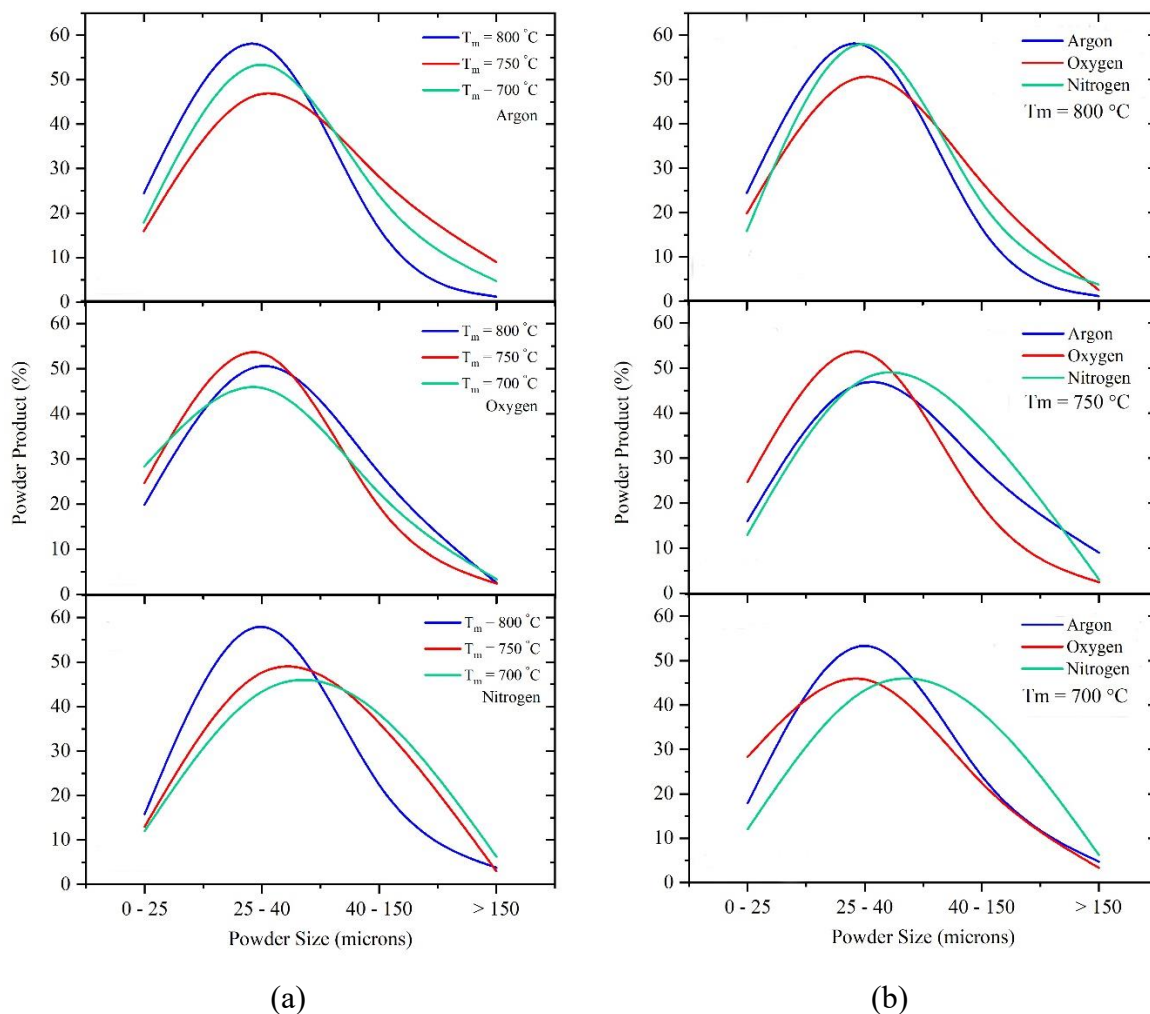(a)   (b)

FIGURE 2. Powder size distribution curves generated by (a) various melting pot temperatures with the same hot gas atomisation and (b) various hot gas atomisation with the same melting pot temperature

PARTICLE SHAPE OF POWDER PRODUCT

The powder particle morphologies were studied with a scanning electron microscope (SEM) for the different types of gas atomisation and melting pot temperatures. A series of unique micrographs can be produced by adjusting the gas atomisation of the tin alloy product. In general, the shape of the powder is strongly influenced by the gas atomisation type and melting pot temperature used.

Figure 3 shows secondary electron (SE) images of a tin alloy powder produced using hot oxygen gas atomisation. It can clearly be seen that the non-spherical particle shape is dominant. This result is in line with Ünal (1992), where to a certain extent the tendency to obtain a spherical shape decreased as the oxygen level increased. Özbilen et al. (1989) stated that the oxygen content described the temperature gradient that occurred between the metal core and the oxide of its surface when this powder was created during the atomisation process. In this case, the different temperature gradients on the droplet surface may have been a factor in the creation of an irregular shape. In addition, the higher temperature gradient can increase the compressive stress and solidification time on the droplet. Furthermore, the DTA result in Figure 8 supports the formation of powder with an irregular shape, which is indicated by an increased number of oxygen molecules.
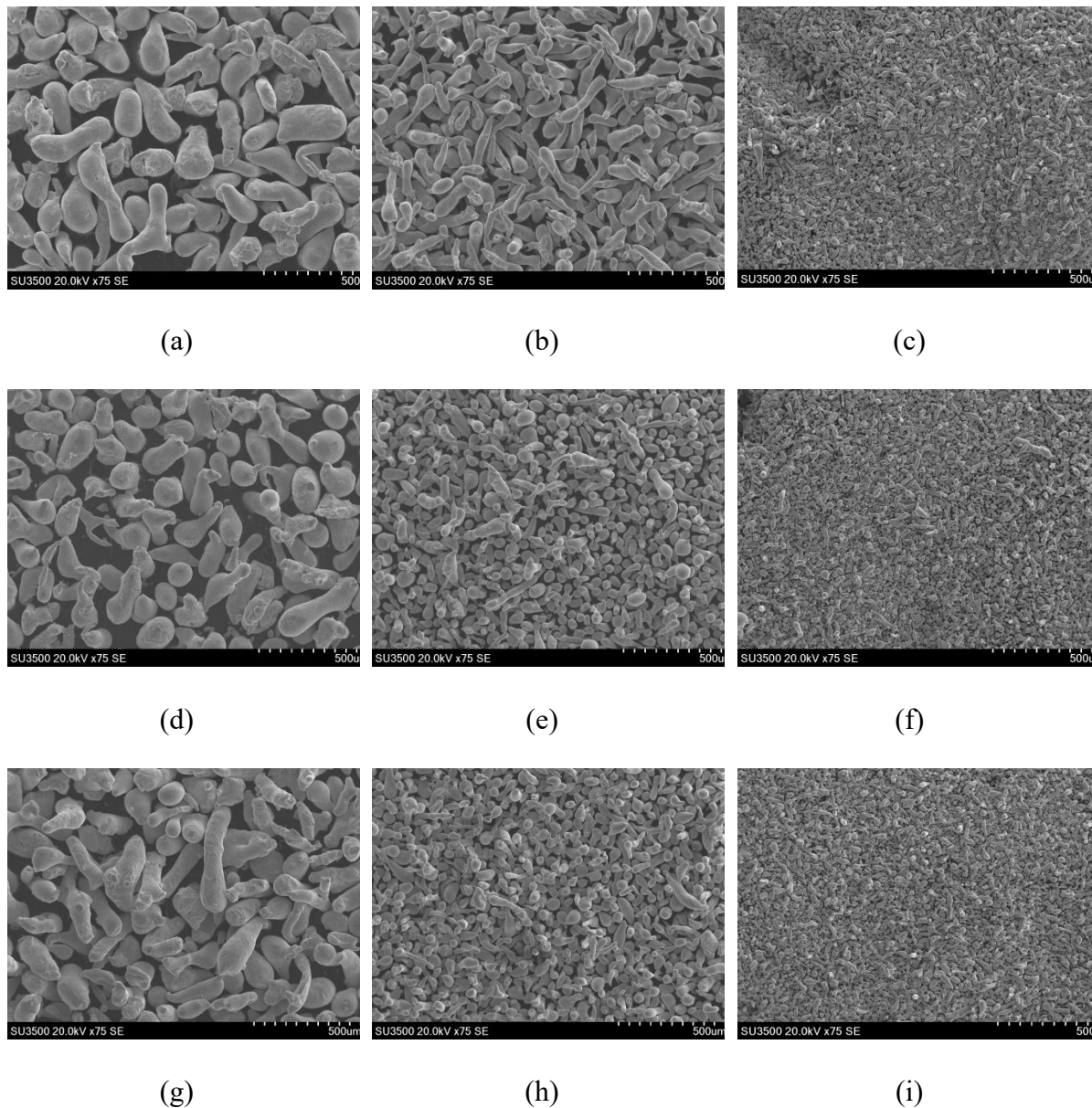

(a)   (b)   (c)

(d)   (e)   (f)

(g)   (h)   (i)

FIGURE 3. SEM micrographs of tin alloy powder with sizes of 40-150 µm, 25-40 µm and 0-25 µm generated by hot oxygen gas atomisation at melting pot temperatures of (a-c) 700 °C, (d-f) 750 °C and (g-i) 800 °C at 75× magnification

The change in the melting pot temperature affects the final powder product. At the melting pot temperature of 700 °C, the powder has the most irregular and elongated particles, as shown in Figure 3(a)-3(c), with an increasing number of spherical particles evident at 750 °C (Figure 3(d)-3(f)). The most spherical particles are found in powder produced at a melting pot temperature of 800 °C (Figure 3(g)-3(i)), although the elongated and irregular shape remains dominant. This phenomenon can be explained by the role of viscosity and surface tension parameters (Huang et al. 2006). The temperature gap between the melting pot and atomisation chamber is lower when the melting pot temperature is higher. This is beneficial in terms of ensuring that the molten tin alloy is in a fully liquid state when impacted by the hot gas atomisation. This can help the molten alloy to solidify in a balanced shape, i.e., spherical.

Figure 4 shows the different morphologies of tin alloy powder with hot nitrogen gas atomisation. There is an increased prevalence of spherical-shaped particles compared to hot oxygen gas atomisation. In general, spherical powder particles can be produced in atomisation systems using an inert gas such as nitrogen, as shown by Ünal (2018). This is because nitrogen does not react with tin, thus producing a more spherical and denser powder product. Figure 4 shows that the number of spherical particles increases in line with the melting pot temperature. As such, Figure 4(a)-4(c) shows that
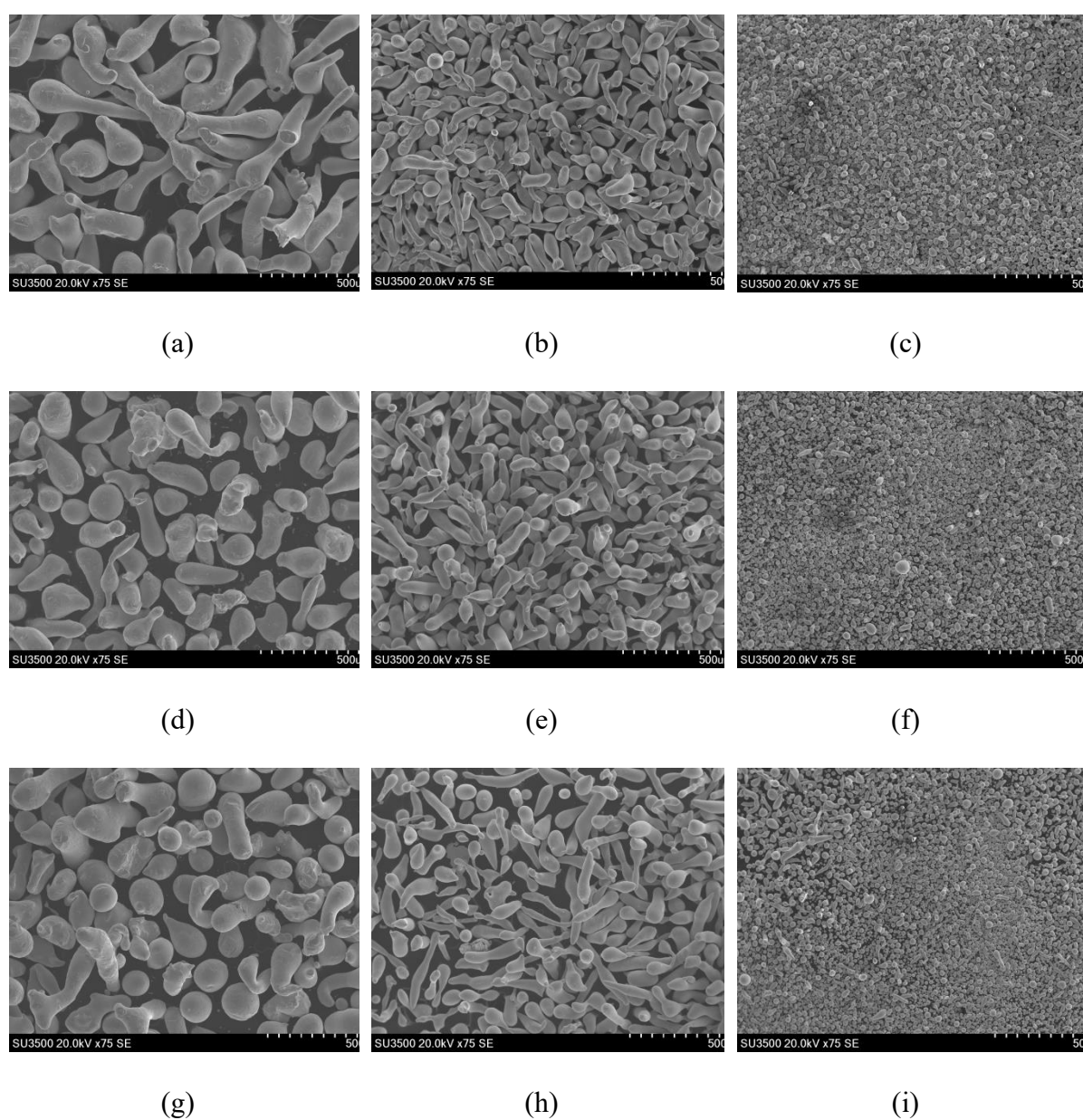

(a) (b) (c)

(d) (e) (f)

(g) (h) (i)

FIGURE 4. SEM micrographs of tin alloy powder with sizes of 40-150 µm, 25-40 µm and 0-25 µm generated by hot nitrogen gas atomisation at melting pot temperatures of (a-c) 700 °C, (d-f) 750 °C and (g-i) 800 °C at 75× magnification

the powder produced at a melting pot temperature of 700 °C contains only a small number of elongated particles. At the melting pot temperature of 750 °C, the powder particles have a less elongated shape and several tailed shapes (Figure 4(d)-4(f)). Furthermore, when the atomisation process is performed at a melting pot temperature of 800 °C, spherical particles become dominant, as shown in Figure 4(g)-4(i).

Compared to the other results, the greatest quantity of spherically shaped particles was obtained using the atomisation process with hot argon gas, as shown in Figure 5. The lower thermal conductivity of argon gas has been found to lead to the fastest rate of solidification among the different atomisation processes (Ünal 2018), thereby producing the most spherical and densest powder. This finding is strengthened in this research, where the atomisation process using hot argon gas generated the most spherical and densest powder compared to the hot nitrogen and oxygen gas. As shown in Figure 5(b), 5(c), 5(e), 5(f), 5(i), and 5(h), the spherical shape is more prevalent in the powder less than 40 µm in size. In contrast, the elongated shape can be observed in powder greater than 40 µm in size. Thus, while the type of gas atomisation is different, the trend remains the same, where the smaller powder particles display a more spherical morphology.

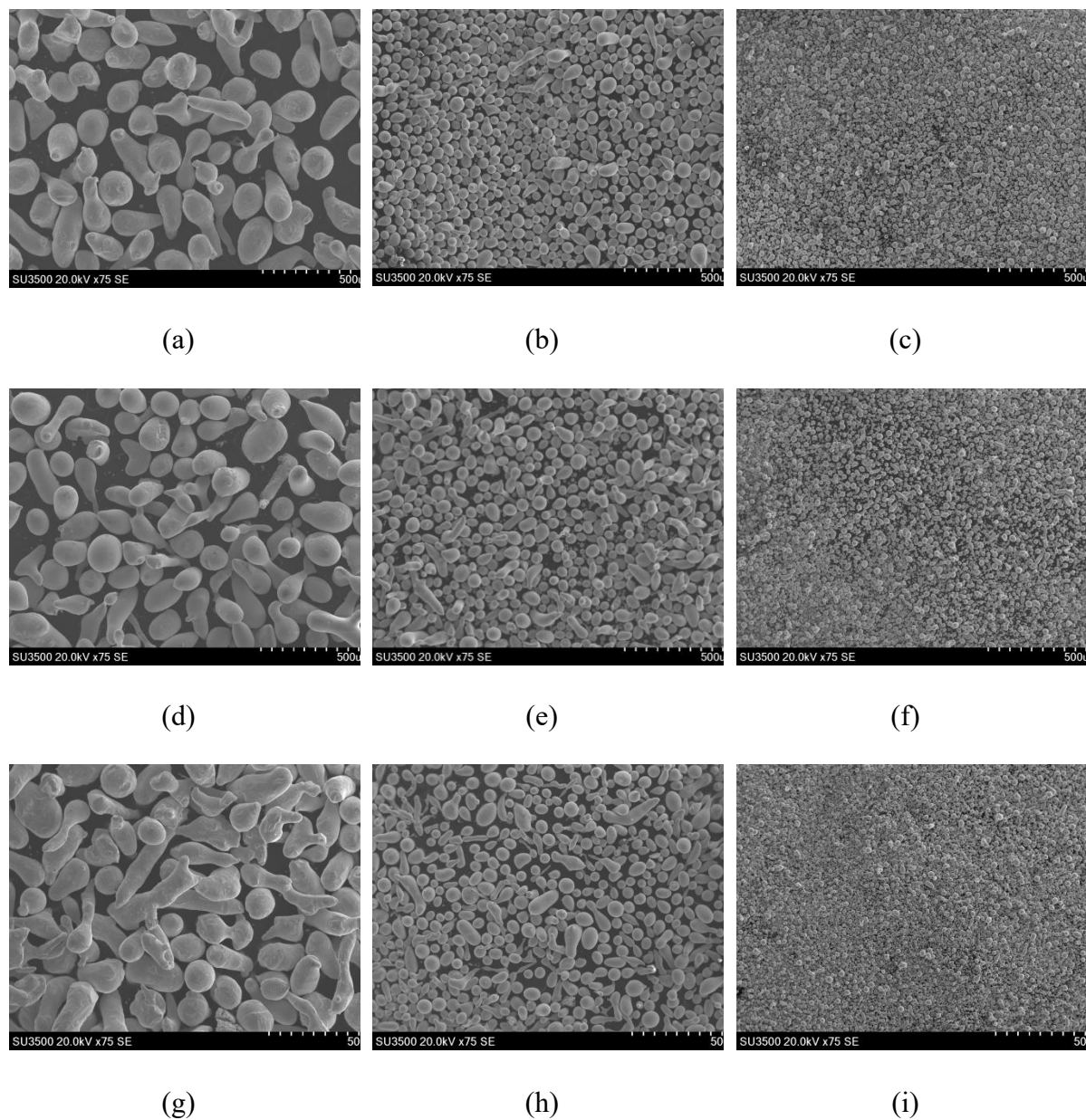(a) (b) (c)

(d) (e) (f)

(g) (h) (i)

FIGURE 5. SEM micrographs of tin alloy powder with sizes of 40-150 µm, 25-40 µm and 0-25 µm generated by hot argon gas atomisation at melting pot temperatures of (a-c) 700 °C, (d-f) 750 °C and (g-i) 800 °C at 75× magnification

The powder formation depends strongly on the gas atomisation type, which is correlated with the specific thermal conductivity of each gas. Herein, the order of specific thermal conductivity is argon (17.81 mW.m^{-1}K^{-1}) < nitrogen (25.93 mW.m^{-1}K^{-1}) < oxygen (26.44 mW.m^{-1}K^{-1}) (Aksoy & Ünal 2006), where lower specific thermal conductivity produces a faster solidification time (Gao et al. 2021). As a result, the powder produced in the argon atmosphere tends to be more spherical and of a higher density than that produced in nitrogen and oxygen atmospheres. This result can be confirmed from the morphology at higher magnification (Figure 7). Herein, the tin alloy powder produced by hot oxygen gas atomisation has a rougher surface and more pores. This roughness and porosity are caused by oxygen molecules that hinder the solidification process during atomisation, resulting in an irregular shape (Urionabarrenetxea et al. 2021). The powder morphology became smoother and less porous as gases with a lower specific thermal conductivity (i.e., nitrogen and argon)

were used. This result aligns with Chen et al. (2018), who reported that inert gas facilitates the formation of powder with a smoother surface and less porosity.

A similar result was obtained when calculating the spherical shape ratio using image-J software, whereby the tin alloy powder produced under hot argon gas atomisation was the most spherical, while the hot oxygen gas atomisation generated the opposite result. Additionally, the tin alloy powder produced at a melting pot temperature of 800 °C generated the most spherical powder, while the melting pot temperature of 750 °C resulted in more spherical powder than 700 °C.

Figure 6(a) shows that hot nitrogen gas atomisation at a melting pot temperature of 800 °C produced a higher ratio of spherically shaped tin alloy powder than the same atomisation at 750 and 700 °C. This ratio of this shape increased dramatically at the 0-25 μm size, while there was little variation among the sizes of 25-40 and 40-150 μm. A similar trend was found concerning hot argon gas atomisation, where spherically shaped
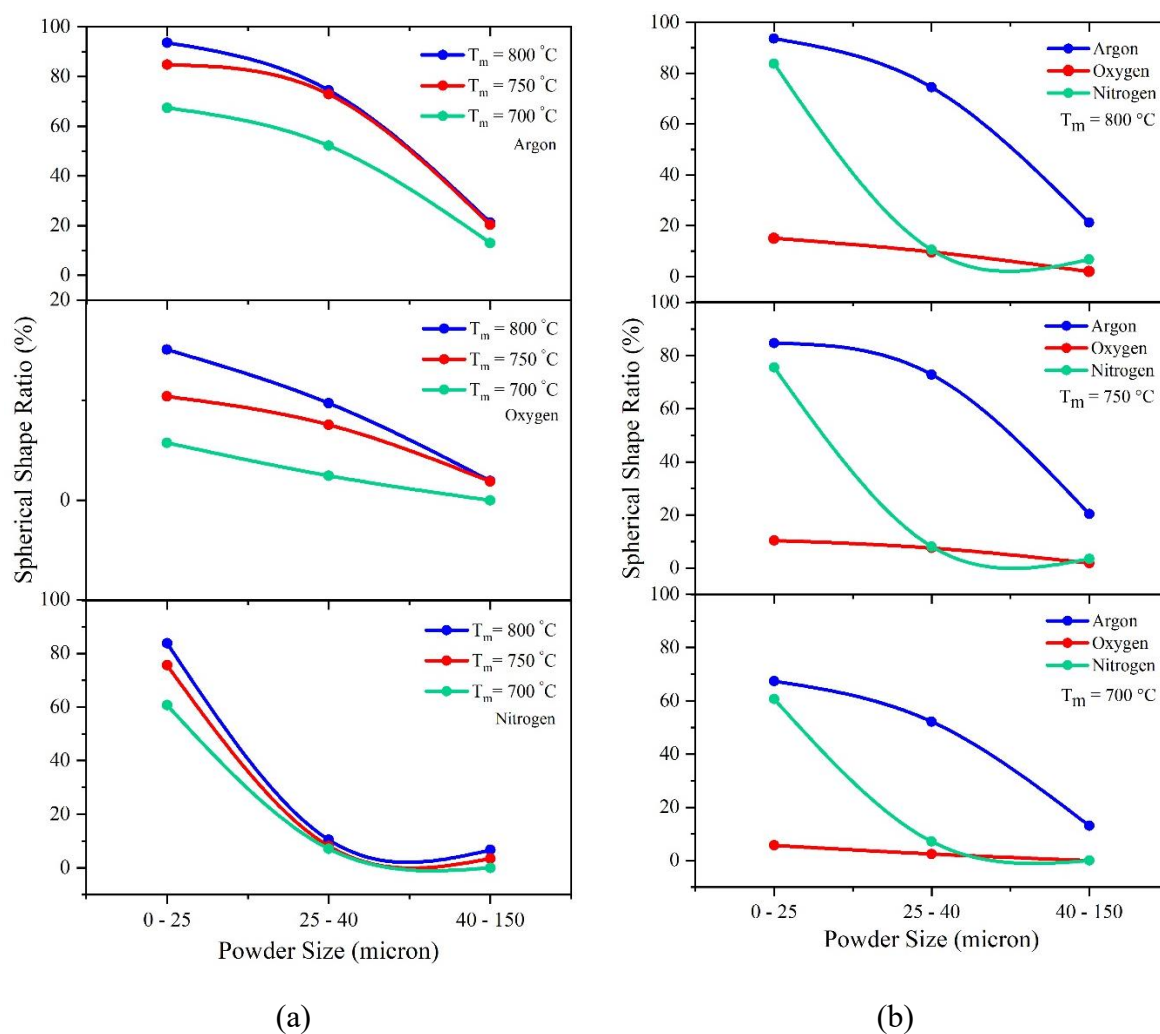

FIGURE 6. Spherical shape ratio curve generated by (a) various melting pot temperatures with the same gas atomisation and (b) various gas atomisation with the same melting pot temperature

tin alloy powder was most commonly observed at a melting pot temperature of 800 °C. While the prevalence of this spherical powder increased sharply from 700 to 750 °C, the difference between 750 and 800 °C was less pronounced, especially for the sizes of 25-40 and 40-150 µm. Moreover, at all melting temperatures, hot oxygen gas atomisation generated a spherical shape ratio of less than 20 %. This indicates that hot oxygen gas atomisation is the least effective in terms of spherical powder production. The availability of spherical

powder increased gradually between the melting pot temperatures of 700, 750 and 800 °C. The spherical shape ratio yielded by hot oxygen gas atomisation at the melting pot temperature of 800 °C was lower than that achieved by hot argon gas atomisation at 700 °C. However, the spherical shape ratio obtained from hot oxygen gas atomisation at all sizes and all melting pot temperatures was similar to that produced by nitrogen gas atomisation at sizes greater than 25 µm for all melting pot temperatures. This phenomenon can be seen clearly in Figure 6(b).
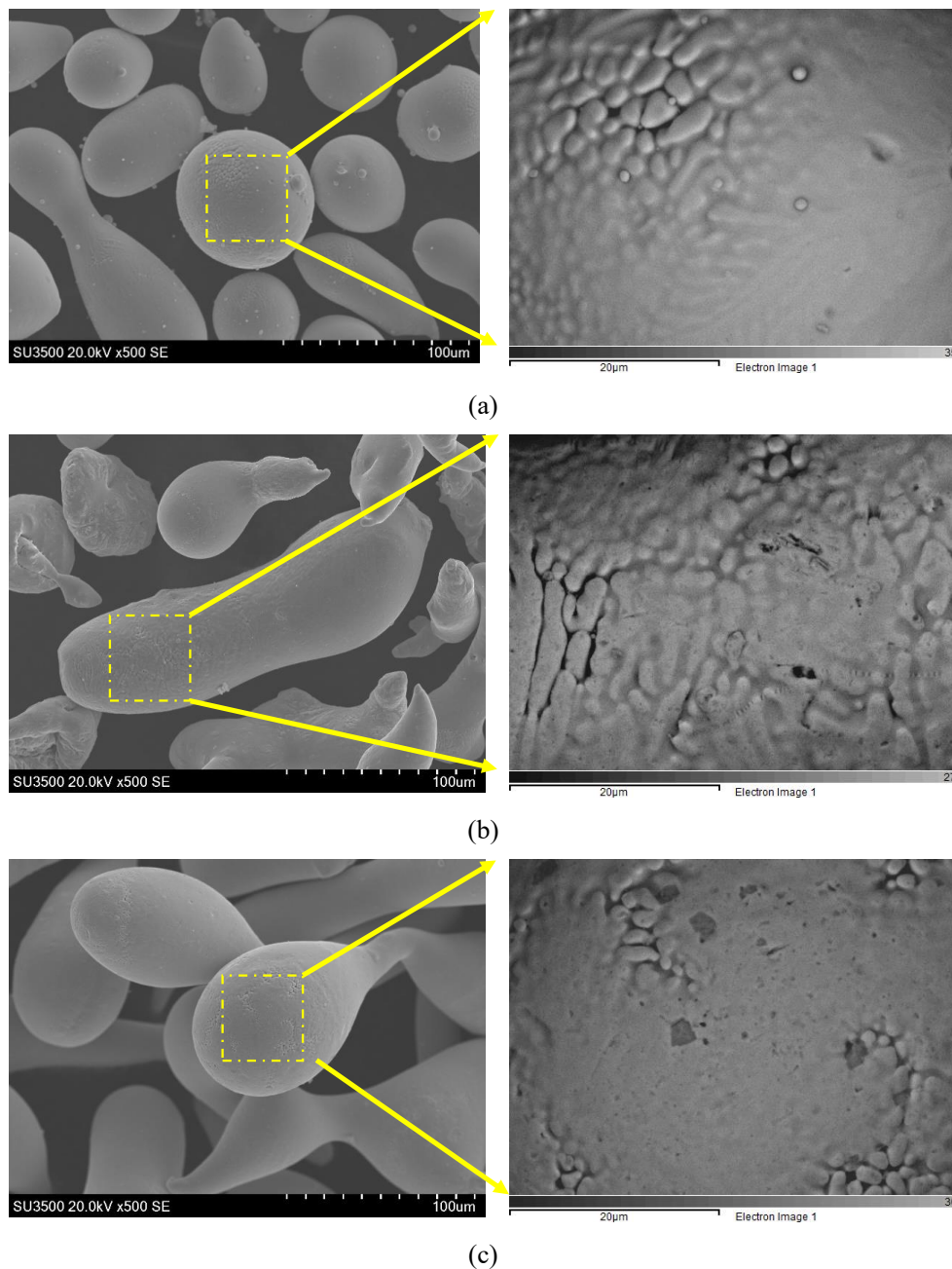

(a)

(b)

(c)

FIGURE 7. Area of EDS for tin alloy powder with a size of 0-25 µm generated by hot (a) argon, (b) oxygen and (c) nitrogen gas atomisation at a melting pot temperature of 800 °C

DENSITY AND THERMAL BEHAVIOUR OF POWDER PRODUCT

Figure 8 shows the DTA of tin alloy powder generated by hot argon, oxygen, and nitrogen gas. The results show that the powder generated using hot argon gas has the highest exothermic area, while the powder generated by hot oxygen gas has the smallest exothermic area. Based on the exothermic area, the enthalpy reaction values (ΔH) in Table 1 shows that powder produced from hot argon gas also has the highest enthalpy reaction, with the lowest value for powder produced from hot oxygen gas. The value of the enthalpy reaction is triggered by the density of each powder, which is also supported by the density data of each powder (Table 2). The powder produced under hot argon gas atomisation has the highest density, while the lowest density occurs with hot oxygen gas atomisation. This can be understood in relation to the powder shape, wherein irregular shapes are dominant. The spherical powder and lower oxygen content thus enhance the density of the powder (Basyir et al. 2020; Zhang et al. 2015).

Based on the DTA results, the powder formed through hot argon gas atomisation has the smallest endothermic area, while the powder formed with hot oxygen gas has the largest endothermic area. This area explicitly indicates the oxygen content of the powder, whereby a larger endothermic area equates to a higher oxygen content. The DTA results of SnO and SnO_2 powder further support this finding, where the SnO_2 has a larger endothermic area than the SnO powder (Figure 9). However, the endothermic area of the powder produced using hot oxygen gas is almost similar to that of the SnO powder. This is because the endothermic area of the SnO powder does not include its melting area (melting temperature of around 1000 °C).
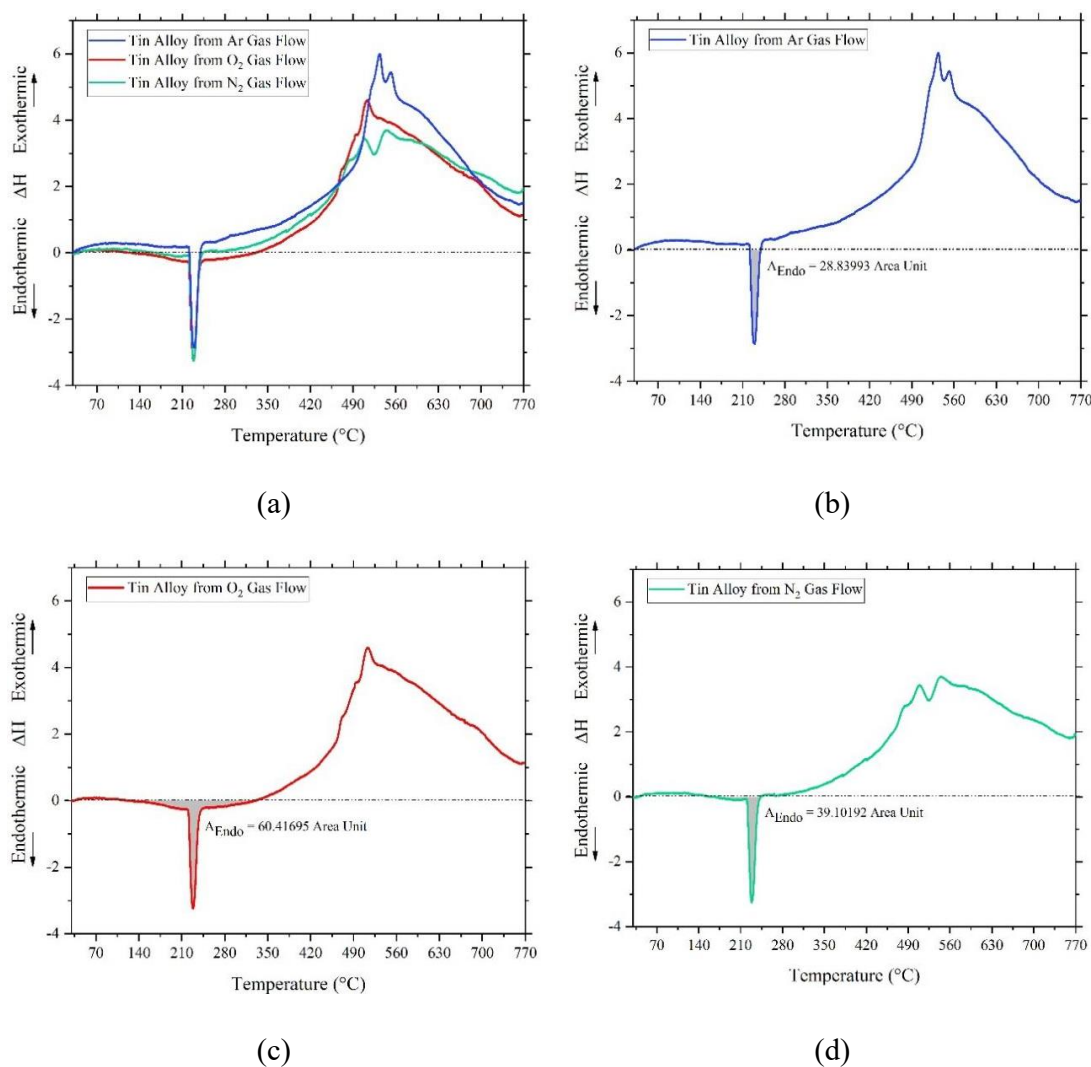

(a)

(b)

(c)

(d)

FIGURE 8. (a) DTA of tin alloy powder generated by hot argon, oxygen and nitrogen gas atomisation, and endothermic area of tin alloy powder generated by hot (b) argon, (c) oxygen and (d) nitrogen gas atomisation

TABLE 1. ΔH of powder generated by hot argon, oxygen and nitrogen gas atomisation

Powder from	Mass (gram)	T_{peak} (°C)	Exo Area (Area unit)	k (cal/mg-Area unit)	ΔH (cal/mg)
Argon gas	0.2634	533	1200.6229	2.0108	9145.5191
Oxygen gas	0.2634	513	953.1413	1.9668	7101.1558
Nitrogen gas	0.2635	545	984.8980	2.0328	7598.1050

TABLE 2. Density of powder generated by hot argon, oxygen and nitrogen gas atomisation

Powder from	m_1 (g)	m_2 (g)	m_3 (g)	m_4 (g)	ρ_{powder} (g/cm³)
Argon gas	12.4278	17.6505	14.4352	19.4028	7.83933
Oxygen gas	12.4278	17.6505	14.4387	19.3679	6.82522
Nitrogen gas	12.4278	17.6505	14.4544	19.3858	6.93032

(a)   (b)
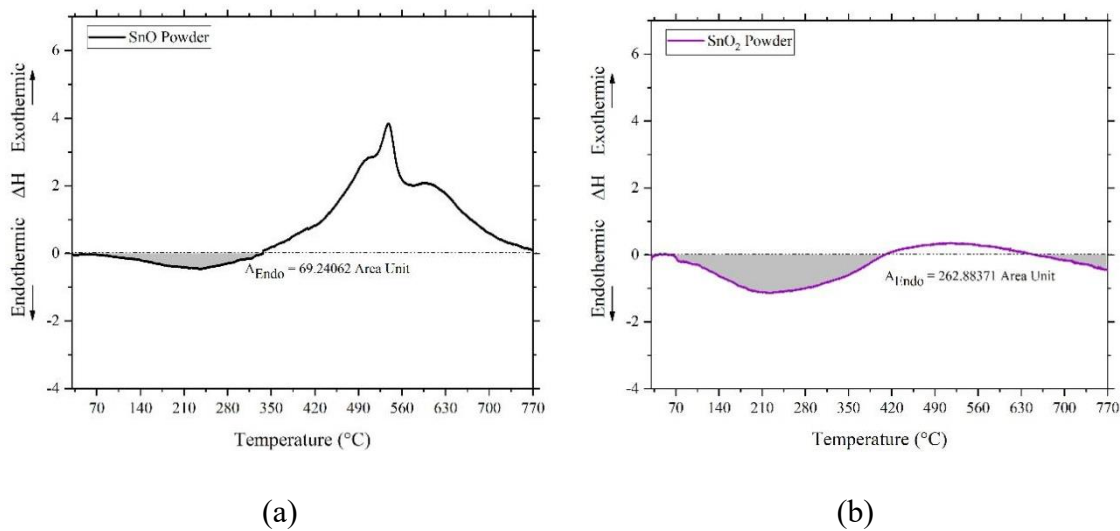
FIGURE 9. DTA and endothermic areas of (a) SnO powder and (b)
SnO_2 powder

PHASE OR ELEMENT OF POWDER PRODUCT

Figure 10 shows the XRD patterns of the powder products (below 25 μm in size) generated by hot argon, oxygen and nitrogen gas atomisation at a melting pot temperature of 800 °C. The results show that these powders consisted of tin (ICCD 04-004-7747) with no peaks as their oxidation product, although the powder was produced by hot oxygen gas. No peaks of Cu, Ni and Ge were observed, which is possibly due to the lower percentages in the tin alloy starting material. However, Cu, Ni and Ge were detected in the EDS elemental analysis results, as shown in Table 3. Ni and Ge were not observed in the powder generated by hot oxygen gas due to the very low weight percentage and non-homogeneous distribution of these elements.
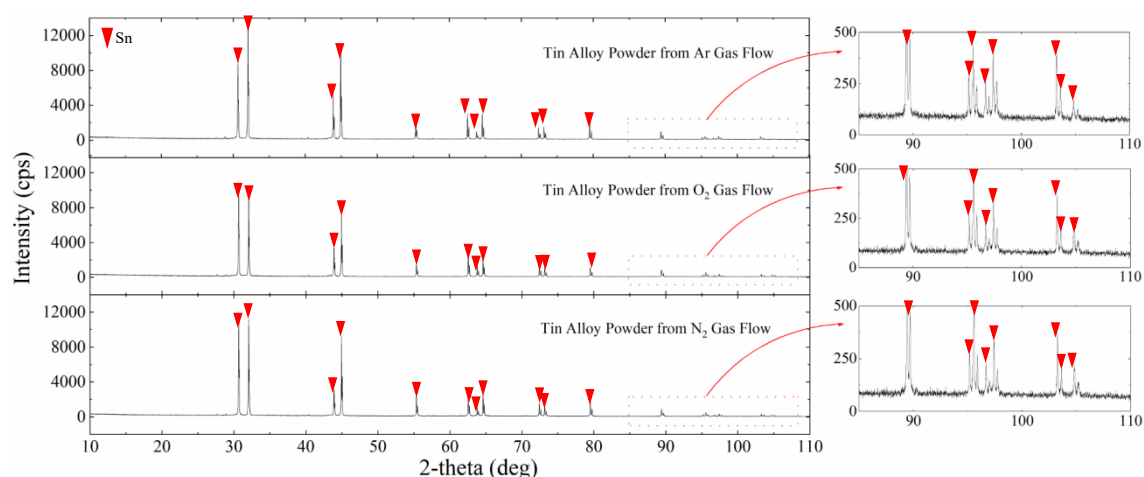
FIGURE 10. Phase of tin alloy powder with a size of 0-25 µm generated by hot
argon, oxygen and nitrogen gas atomisation at a melting pot temperature of 800 °C

TABLE 3. EDS result of powder generated by hot argon, oxygen and nitrogen gas atomisation

Powder from	Composition			
	Sn (wt.%)	Cu (wt.%)	Ni (wt.%)	Ge (wt.%)
Argon gas	99.14	0.71	0.06	0.09
Oxygen gas	98.92	1.08	-	-
Nitrogen gas	99.03	0.86	0.01	0.1

Conclusions

This study has investigated the effect of using different hot gas types and melting pot temperatures in the gas atomisation process on the characteristics of powder products. Based on the findings, the following conclusions can be drawn: Gas atomisation using hot oxygen at the melting pot temperature of 700 °C generated more powder product below 25 µm in size than the melting pot temperature of 800 °C, where the reverse result was produced by hot argon and nitrogen gas atomisation. Hot oxygen gas atomisation generated the largest quantity of powder below 25 µm in size. Gas atomisation using hot argon generated the largest quantity of spherical powder product and the prevalence of the spherical shape increased at the melting pot temperature of 800 °C. The powder product generated using hot argon gas atomisation had the greatest density and the smallest endothermic area or lowest oxygen content. The powder products obtained from hot argon and nitrogen gas consist of similar elements to the starting materials.

REFERENCES

Akkas, M. & Boz, M. 2019. Investigation of the compressibility and sinterabilty of AZ91 powder production and particle production by gas atomisation method. *Journal of Magnesium and Alloys* 7(3): 400-413. https://doi.org/10.1016/j.jma.2019.05.007

Aksoy, A. & Ünal, R. 2006. Effects of gas pressure and protrusion length of melt delivery tube on powder size and powder morphology of nitrogen gas atomised tin powders. *Powder Metallurgy* 49(4): 349-354. https://doi.org/10.1179/174329006X89425

Anderson, I.E. & Terpstra, R.L. 2002. Progress toward gas atomization processing with increased uniformity and control. *Materials Science and Engineering A* 326(1): 101-109. https://doi.org/10.1016/S0921-5093(01)01427-7

Basyir, A., Aryanto, D., Wismogroho, A.S. & Widayatno, W.B. 2020. Effect of hot isostatic pressing method to enhance quality of tin powder. In *AIP Conference Proceedings*. AIP Publishing LLC. 2256(030021): 1-9. https://doi.org/10.1063/5.0014653

Chen, G., Zhao, S.Y., Tan, P., Wang, J., Xiang, C.S. & Tang, H.P. 2018. A comparative study of Ti-6Al-4V powders for additive manufacturing by gas atomization, plasma rotating electrode process and plasma atomization. *Powder Technology* 333: 38-46. https://doi.org/10.1016/j.powtec.2018.04.013

Chhabra, R.P. & Sheth, D.K. 1990. Viscosity of molten metals and its temperature dependence. *International Journal of Material Research* 81(4): 264-271. https://doi.org/10.1515/ijmr-1990-810408

Drellishak, K.S., Aeschliman, D.P. & Cambel, A.B. 1964. *Tables of Thermodynamic Properties of Argon, Nitrogen, and Oxygen Plasmas*. Illinois: Arnold Engineering Development Center.

Feng, G., Jiao, K., Zhang, J. & Gao, S. 2021. High-temperature viscosity of ironcarbon melts based on liquid structure: The effect of carbon content and temperature. *Journal of Molecular Liquids* 330: 115603. https://doi.org/10.1016/j.molliq.2021.115603.

Gao, C.F., Xiao, Z.Y., Zou, H.P., Liu, Z.Q., Chen, J., Li, S.K. & Zhang, D.T. 2019. Characterization of spherical $AlSi_{10}Mg$ powder produced by double-nozzle gas atomization using different parameters. *Transactions of Nonferrous Metals Society of China* 29(2): 374-384. https://doi.org/10.1016/S1003-6326(19)64947-2

Gao, M.Z., Ludwig, B. & Palmer, T.A. 2021. Impact of atomization gas on characteristics of austenitic stainless steel powder feedstocks for additive manufacturing. *Powder Technology* 383: 30-42. https://doi.org/10.1016/j.powtec.2020.12.005

Huang, Z., Czisch, C., Schreckenberg, P., Büllesfeld, F. & Fritsching, U. 2006. Technical note: Powder production by gas atomization of bioglass melt. *Particle and Particle Systems Characterization* 22(5): 345-351. https://doi.org/10.1002/ppsc.200500966

Kaysser, W.A. & Weise, W. 2000. Powder metallurgy and sintered materials. *Ullmann's Encyclopedia of Industrial Chemistry*. https://doi.org/10.1002/14356007.a22_105

Kong, C.J., Brown, P.D., Harris, S.J. & McCartney, D.G. 2007. Analysis of microstructure formation in gas-atomised Al-12 Wt.% Sn-1 Wt.% Cu alloy powder. *Materials Science and Engineering A* 454-455: 252-259. https://doi.org/10.1016/j.msea.2006.11.050

Metz, R., Machado, C., Houabes, M., Pansiot, J., Elkhatib, M., Puyanē, R. & Hassanzadeh, M. 2008. Nitrogen spray atomization of molten tin metal: powder morphology characteristics. *Journal of Materials Processing Technology* 189(1-3): 132-137. https://doi.org/10.1016/j.jmatprotec.2007.01.014

Minagawa, K., Kakisawa, H., Osawa, Y., Takamori, S. & Halada, K. 2005. Production of fine spherical lead-free solder powders by hybrid atomization. *Science and Technology of Advanced Materials* 6(3-4): 325-329. https://doi.org/10.1016/j.stam.2005.03.010

Neikov, O.D., Naboychenko, S.S. & Yefimov, N.A. 2009. *Handbook of Non-Ferrous Metal Powders: Technologies and Applications,* edited by Neikov, O.D., Naboychenko, S.S. & Dowson, G. Amsterdam: Elsevier Ltd.

Nishimura, S., Matsumoto, S. & Terashima, K. 2002. Variation of silicon melt viscosity with boron addition. *Journal of Crystal Growth* 237-239: 1667-1670. https://doi.org/10.1016/S0022-0248(01)02317-X

Özbilen, S., Ünal, A. & Sheppard, T. 1996. Influence of liquid metal properties on particle size of inert gas atomised powders. *Powder Metallurgy* 39(1): 44-52. https://doi.org/10.1179/pom.1996.39.1.44

Özbilen, S., Ünal, A. & Sheppard, T. 1989. Influence of oxygen on morphology and oxide content of gas atomized aluminium powders. In *Physical Chemistry of Powder Metals: Production and Processing*. pp. 489-505.

Pan, H., Ji, H., Liang, M., Zhou, J. & Li, M. 2019. Size-dependent phase transformation during gas atomization process of Cu-Sn alloy powders. *Materials* 12(2): 245-257. https://doi.org/10.3390/ma12020245

Plookphol, T., Wisutmethangoon, S. & Gonsrang, S. 2011. Influence of process parameters on SAC305 lead-free solder powder produced by centrifugal atomization. *Powder Technology* 214(3): 506-512. https://doi.org/10.1016/j.powtec.2011.09.015

Tanaka, T. & Hara, S. 1997. Surface tension and viscosity of liquid iron alloys. *Materia Japan* 36(1): 47-54. https://doi.org/10.2320/materia.36.47

Ünal, A. 1992. Rapid solidification of magnesium by gas atomization. *Materials and Manufacturing Processes* 7(3): 441-461. https://doi.org/10.1080/10426919208947431

Ünal, A. 2018. Production of rapidly solidified aluminium alloy powders by gas atomisation and their applications. *Powder Metallurgy* 33(1): 53-64. https://doi.org/10.1179/pom.1990.33.1.53

Urionabarrenetxea, E., Avello, A., Rivas, A. & Martín, J.M. 2021. Experimental study of the influence of operational and geometric variables on the powders produced by close-coupled gas atomisation. *Materials & Design* 199: 109941. https://doi.org/10.1016/j.matdes.2020.109441

Vandel, E., Vaasma, T. & Sugita, S. 2020. Application of image analysis technique for measurement of sand grains in sediments. *MethodsX* 7: 100981. https://doi.org/10.1016/j.mex.2020.100981

Vippola, M., Valkonen, M., Sarlin, E., Honkanen, M. & Huttunen, H. 2016. Insight to nanoparticle size analysis - novel and convenient image analysis method versus conventional techniques. *Nanoscale Research Letters* 11: 1-9. https://doi.org/10.1186/s11671-016-1391-z

Wisutmethangoon, S., Plookphol, T. & Sungkhaphaitoon, P. 2011. Production of SAC305 powder by ultrasonic atomization. *Powder Technology* 209(1-3): 105-111. https://doi.org/10.1016/j.powtec.2011.02.016

Xie, J.W., Zhao, Y.Y. & Dunkley, J.J. 2004. Effects of processing conditions on powder particle size and morphology in centrifugal atomisation of tin. *Powder Metallurgy* 47(2): 168-172. https://doi.org/10.1179/003258904225015482

Younglove, B.A. & Olien, N.A. 1985. *Tables of Industrial Gas Container Contents and Density for Oxygen, Argon, Nitrogen, Helium, and Hydrogen*. Washington DC: United States Government Printing Office.

Zhang, L., Chen, X., Li, D., Chen, C., Qu, X., He, X. & Li, Z. 2015. A comparative investigation on MIM418 superalloy fabricated using gas- and water-atomized powders. *Powder Technology* 286: 798-806. https://doi.org/10.1016/j.powtec.2015.09.023

Zhang, L.P. & Zhao, Y.Y. 2017. Particle size distribution of tin powder produced by centrifugal atomisation using rotating cups. *Powder Technology* 318: 62-67. https://doi.org/10.1016/j.powtec.2017.05.038

Zhao, X., Xu, J., Zhu, X. & Zhang, S. 2008. Effect of closed-couple gas atomization pressure on the performances of Al-20Sn-1Cu powders. *Rare Metals* 27(4): 439-443. https://doi.org/10.1016/S1001-0521(08)60159-X

*Corresponding author; email: abdulbasyir037@gmail.com